Novel Bis Maleimide Derivatives Containing Azo Group: Synthesis, Corrosion Inhibition, and Theoretical Study

Hawraa Kareem Dhaef, Rafid Humaidan Al-Asadi, Ashwaq Abood Shenta, and Mohammed Khalaf Mohammed*

Department of Chemistry, College of Education for Pure Science, University of Basrah, Basrah 61004, Iraq

* ***Corresponding author:***

email: mohammed.khalaf@uobasrah.edu.iq

Received: March 10, 2021
Accepted: September 14, 2021

DOI: 10.22146/ijc.64614

Abstract: *Novel derivatives of heterocyclic azo compounds have been synthesized through a free catalyst reaction. The structures of the synthesized compounds were confirmed by using different techniques such as ^{1}H-NMR, ^{13}C-NMR, and mass spectroscopy. The prepared derivatives were evaluated as corrosion inhibitors for mild steel after the inhibitory performance toward mild steel in 0.1 M HCl solution. The prepared derivatives, i.e. (1,1'-(((1E,1'E)-1,4-Phenylenebis(diazene-2,1-diyl))bis(4-methyl-3,1-phenylene))bis(1H-pyrrole-2,5-dione)) **1** and (1,1'-(((1Z,1'Z)-(Oxybis (4,1-phenylene))bis(diazene-2,1-diyl))bis(4-methyl-3,1-phenylene))bis(1H-pyrrole-2,5 -dione)) **2** showed inhibition efficiency 89.22% and 91.30%, respectively at concentration 1×10^{-3} M. The isotherm adsorptions of these derivatives were found to obey Langmuir model. Furthermore, Density functional theory was used for theoretical estimation of the HOMO, LUMO, and other chemical quantum parameters. The results indicated that the synthesized derivatives displayed a corrosive inhibitory property in which derivative **2** was more effective than derivative **1**. In addition, the theoretical results were in agreement with the experimental data.*

Keywords: *azo compounds; N-(4-hydroxylpheneyl) maleimide; Tafel curve; corrosion inhibition; theoretical study*

■ INTRODUCTION

Corrosion is seen to be a major problem that restricts the widespread use of metallic materials. Corrosion-related damage causes an increase in the maintenance cost. Thus, there is a greater need to protect the materials used. Many researchers have attempted to develop methods for decreasing corrosion on metals [1-2]. The metallic materials react with their surrounding media based on the electrochemical corrosion process. Various environmental conditions such as acidity, salinity, moisture, and aeration are responsible for causing the corrosion of iron or iron alloy materials. Corrosion can deteriorate materials properties such as chemical, physical and mechanical properties [3-4].

One method to achieve this purpose includes using organic inhibitors that could effectively decrease or prevent the corrosion effects of metals and metallic alloys. Organic compounds can create a protective layer that reduces or prevents the penetration of many corrosive factors from reaching metal surfaces. Therefore, the success of this method reduces the formation of defects on metal surfaces. The organic inhibitors used to prevent steel surface corrosion include organic compounds that contain sulfur, nitrogen, and/or oxygen atoms [5-6].

Azo compounds are an important class of organic compounds that are versatile for synthetic organic compounds. Azo compounds can be used in several applications [7], for instance, textiles, leather, cosmetics, pharmaceutical reagents, and even corrosion inhibitors [8] such as used it as corrosion inhibitors for carbon steel [9-10], mild steel [11-12], and aluminum [13-15]. The protective methods involved a chemical reaction between the azo group and the various substituted aromatic bonds that exist on the metallic surfaces. This process reveals an intense color to the compounds over the full visible range. Moreover, these chemical reactions

also enhance the metals' stability, require less production cost, and use uncomplicated synthetic processes [8-11].

We have synthesized novel maleimide derivatives and tested their efficiency against the carbon steel material in this work. These derivatives were dissolved in 0.1 M HCl and tested to evaluate their corrosion inhibitory efficiency using a potentiodynamic polarization technique. In addition, computer simulations were conducted to calculate some quantum chemical parameters values to study the relationship between theoretical and practical properties.

■ EXPERIMENTAL SECTION

Materials

Chemicals and solvents were ordered from Sigma-Aldrich (USA). The progress of reactions was monitored by using thin-layer chromatography (TLC) for all the synthesized compounds using pre-coated silica gel 60, UV 254 TLC plates. The ^{1}HNMR and ^{13}CNMR spectra were recorded on a Bruker Inovo AV-400 spectrometer (Iran), using DMSO-d_6 as a solvent. The protons for the decoupling values (*J*) are expressed in Hz, and the melting points of the compounds were measured with the help of capillary tubes using a Gallenkamp melting point apparatus. The accurate mass spectra of the synthesized compounds were run on a JEOL JMS-5X 10217 in the EI genre (Iran).

Procedure

Synthesis of 1,1'-(((1E,1'E)-1,4-phenylenebis(diazene-2,1-diyl))bis(4-methyl-3,1-phenylene))bis(1H-pyrrole-2,5-dione) (1)

A cooled solution of benzene-1,4-diamine (0.01 mol) dissolved in a dilute HCl solution (conc. HCl:H_2O, 1:1 v/v) was kept in an ice bath (≤ 5 °C). $NaNO_2$ (0.02 mol) dissolved in water (10 mL) was added dropwise to the above solution. This mixture was continually stirred under the ice bath. To the above content, N-(4-methyl phenyl) maleimide) (0.02 mol) was added according to the references [14–16]. The resulting mixture was dissolved in NaOH solution (10% wt/v, 20 mL) at 5 °C. The resulting mixture was chilled in an ice bath and additionally stirred for 20 min. The resulting precipitate was then filtered and recrystallized from glacial acetic acid and washed with methanol to remove the traces of glacial acetic acid. Finally, a precipitate formed that was filtered, washed with distilled water, and the desired product was dried in the oven at 50 °C for 24 h.

Brown solid, yield 85%, m.p 150–153 °C. ^{1}H-NMR (500 MHz, DMSO-d_6) δ (ppm): 2.25, s (6H, CH_3), 6.30, d (2H, *J* = 10 MHz, CH=CH), 6.46, d (2H, *J* = 10 MHz, CH=CH), 7.13–7.52, m (10H, Ar-H). ^{13}C-NMR (125 MHz) δ (ppm): 16.71, 104.51, 117.78, 119.95, 127.48, 129.36, 129.52,131.99, 135.96, 171.76, MS $[EI]^+$ m/z 504$[M]^+$.

Synthesis of 1,1'-(((1Z,1'Z)-(oxybis(4,1-phenylene))bis(diazene-2,1-diyl))bis(4-methyl-3,1-phenylene))bis(1H-pyrrole-2,5-dione) (2)

A cooled solution of 4,4'-oxydianiline (0.01 mol) dissolved in a dilute HCl solution (conc. HCl:H_2O, 1:1 v/v) was kept in an ice bath (≤ 5 °C). $NaNO_2$ (0.02 mol) dissolved in water (10 mL) was added dropwise to the above solution. This mixture was continually stirred under the ice bath. To the above content, N-(4-methyl phenyl) maleimide) (0.02 mol) was added according to the references [14-16]. The resulting mixture was dissolved in NaOH solution (10% wt/v, 20 mL) at 5 °C. The resulting mixture was chilled in an ice bath and additionally stirred for 20 min. The resulting precipitate was then filtered and recrystallized from glacial acetic acid and washed with methanol to remove the traces of glacial acetic acid. Finally, the desired product was dried in the oven at 50 °C for 24 h.

Brown solid; yield 79%, m.p. 178–180 °C, ^{1}H-NMR (500 MHz, DMSO) δ (ppm): 2.26, s (6H, CH_3), 6.30, d (2H, *J* = 10 MHz, CH=CH), 6.46, d (2H, *J* = 10 MHz, CH=CH), 7.13–7.52, m (14H, Ar-H). ^{13}C-NMR (125 MHz, DMSO) δ (ppm): 16.70, 104.01, 117.77, 118.01, 119.86, 127.38, 128.47, 130.98, 131.18, 135.47, 135.89, 171.65, MS $[EI]^+$ m/z 540 $[M]^+$.

Theoretical calculations

The chemical structure of studied compounds has been drawn by ChemDraw-2014 program in a 2D format and saved as MDL Molfile. Then the file was opened in the Material Studio-DMol3 ver. 5.5 Software

program. The synthesized compounds' geometry optimization and energies calculation were performed using density functional theory (DFT). Becke exchange plus Lee-Yang-Parr correlation (BLYP) and Double Numerical plus d-functions (DND) as the basis set have been applied on the synthesized compounds. The BLYP/DND level has been shown to be suitable for bismaleimide compounds where the results calculated are consistent with the corresponding experimental results [17]. Material Studio-DMol3 ver. 5.5 Software was used to extract the output files. Energy values of the extracted molecular orbital were determined to calculate E_{LUMO} and E_{HOMO} using the calculated values of numerous quantum chemical parameters according to the following Eq. (1-7) [18]. The calculations were made using DELL laptop with a dual-core processor and Ram 4 Giga.

$$\text{Ionization potential (IP)} = -E_{HOMO} \quad (1)$$

$$\text{Electron affinity (EA)} = -E_{LUMO} \quad (2)$$

$$\text{Electronegativity } (\chi) = -1/2\left(E_{HOMO} + E_{LUMO}\right) \quad (3)$$

$$\text{Chemical hardness } (\eta) = -1/2\left(E_{HOMO} - E_{LUMO}\right) \quad (4)$$

$$\text{Global electrophilicity } (\omega) = \chi^2/2\eta \quad (5)$$

$$\text{Absolute softness } (\sigma) = 1/\eta \quad (6)$$

$$\text{Number electrons transferred } (\Delta N) = \chi_{Fe} - \chi_{inh}/2\left(\eta_{Fe} + \eta_{inh}\right) \quad (7)$$

■ RESULTS AND DISCUSSION

Chemistry

In this work, diazonium salts were prepared by diazonation of benzene-1,4-diamine and 4,4'-oxydianiline in the presence of dilute HCl acid and sodium nitrite. The resulted diazonium compounds were coupled with *N*-(4-methylphenyl) maleimide to synthesize compounds **1** and **2**, as shown in Scheme 1.

The structure of these compounds **1** and **2** was confirmed by their ^{1}H-NMR, ^{13}C-NMR, and mass spectroscopy. The ^{1}H-NMR spectra show two distinct doublets δ = 6.30 and 6.46 ppm for alkene group (CH=CH) at the expected regions. In addition, one singlet signal was noted at δ = 2.25 ppm for compound **1** and δ = 2.26 ppm for compound **2** attributed to the protons of methyl groups. The other aromatic protons appeared as multiplet signals between δ = 7.13–7.64 ppm and 7.13–7.52 ppm for compounds **1** and **2**, respectively.

On the other hand, the ^{13}C-NMR spectra displayed the following signals, which confirmed the structure of the synthesized compounds: 171.76 and 171.65 ppm (C=O); 135.89 and 135.96 ppm (HC=CH); 135.74 ppm (C–O) for compound **2**; 131.99-104.01 ppm (C=C, aromatics), and 16.71 and 16.70 ppm (CH_3). Moreover, the mass spectra of compounds indicated the presence of molecular ion peak as a base peak at m/z 504 for compound **1** and m/z 540 for compound **2**.

Polarization Measurements

Fig. 1 depicts the polarization behavior of mild steel material in 0.1 M HCl, either in the presence or absence of the compound **1** and **2** (as inhibitors) at 25 °C. The results indicated that the cathodic and anodic reactions using the mild steel electrode corrosion were decreased when the inhibitor concentration was increased. Hence, it was concluded that the inhibitor

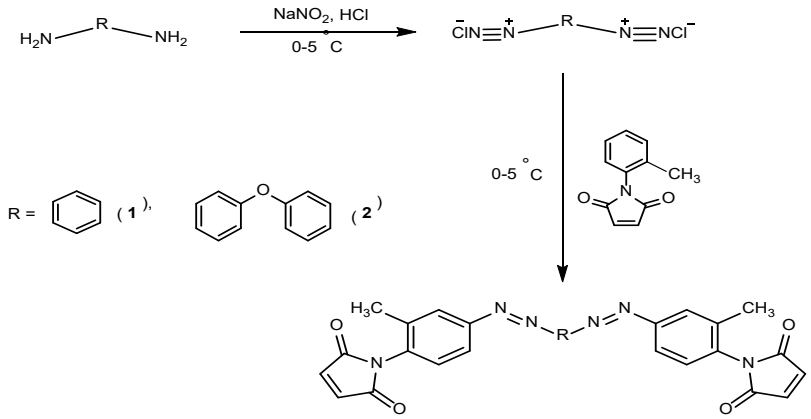

Scheme 1. Chemical structure of the synthesized inhibitors

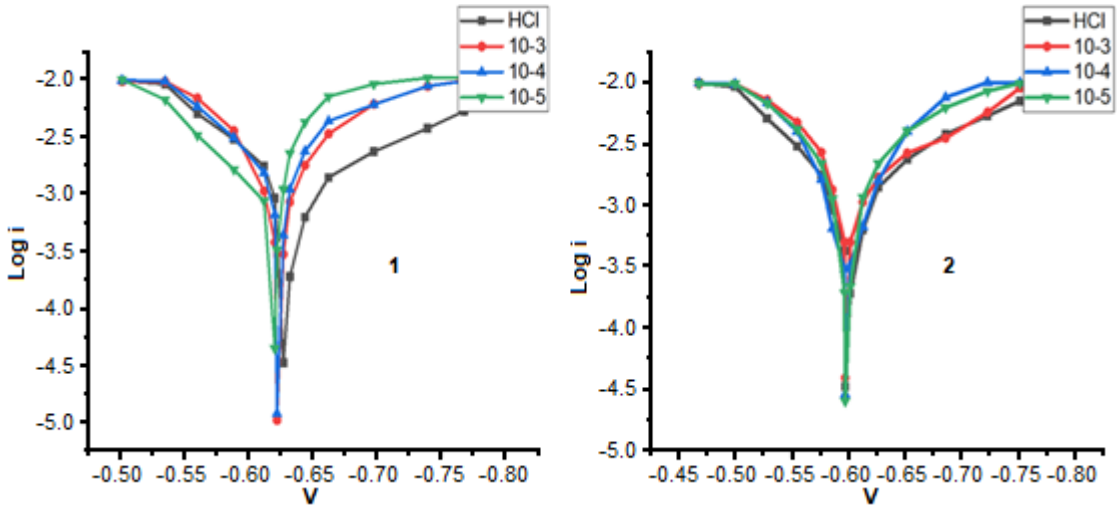

Fig 1. Galvanostatic polarization curves of mild-steel in 0.1 M HCl in the different concentrations of inhibitors **1** and **2** at 25 °C

addition reduced the anodic dissolution and decreased the hydrogen evolution.

The electrochemical parameters such as corrosion current density (I_{corr}), corrosion potential (E_{corr}), cathodic Tafel constant (βc), and anodic Tafel constant (βa) and corrosion rate (CR) were estimated by using Tafel plots [19,20]. The results of different electrochemical parameters are shown in Table 1 and 2. The addition of the corrosion inhibitor reduced the current density. The maximum decrease in the I_{corr} value was observed for compounds **1** and **2** in a concentration of 1×10^{-3}. The E_{corr} values observed for compounds **1** and **2** showed a slight change towards the anode and cathodic directions, exhibiting no specific trend upon dissolution in 0.1 M HCl. The result indicated that the compounds behave act as a mixed inhibitory behavior. These inhibitory compounds changed the cathodic and anodic Tafel slopes, indicating that the inhibitors affected the cathodic and anodic reaction mechanisms without blocking any reaction mechanisms or any reaction sites

Table 1. The corrosion parameters for the corrosion of mild steel in 0.1 M HCl by galvanostatic polarization in presence inhibitor **1**

Conc. (M)	CR (mpy)	I_{corr} (A)	E_{corr} (V)	βc (A/V)	βa (A/V)	IE%	θ
0.00	3.383	0.00233	-0.739	-2.884	5.951	_	_
1×10^{-5}	2.227	0.00030	-0.618	-5.048	3.748	87.09	0.8709
1×10^{-4}	2.211	0.00020	-0.625	-4.996	4.352	87.77	0.8777
1×10^{-3}	1.812	0.00025	-0.624	-4.908	6.300	89.22	0.8922

Table 2. The corrosion parameters for the corrosion of mild steel in 0.1 M HCl by galvanostatic polarization in presence inhibitor **2**

Conc. (M)	CR (mpy)	I_{corr} (A)	E_{corr} (V)	βc (A/V)	βa (A/V)	IE%	θ
0.00	3.383	0.00233	-0.739	-2.884	5.951	-	-
1×10^{-5}	1.584	0.00023	-0.684	-4.698	6.293	90.08	0.9008
1×10^{-4}	1.580	0.00020	-0.597	-5.190	6.368	90.60	0.9060
1×10^{-3}	1.221	0.00020	-0.620	-5.064	6.554	91.30	0.9130

on the mild steel surfaces. The inhibition efficiency (IE%) and degree of coverage on the metal surface (θ) were calculated by using the following Eq. (8) and (9) [21]:

$$IE\% = \left[I_{corr} - \frac{I_{corr}(inh)}{I_{corr}} \right] \times 100 \quad (8)$$

$$\theta = \left[1 - \frac{I_{corr}(inh)}{I_{corr}} \right] \quad (9)$$

where I_{corr} and I_{corr} (inh) are the corrosion current in the presence and absence of inhibitor, respectively.

Adsorption Isotherm

Adsorption isotherm is useful to understand the inhibition mechanism that involves in a corrosion chemical reaction [22]. The common adsorption isotherms are represented as Freundlich, Frumkin, Langmuir, and Temkin isotherm models. In our work, the data showed a good consistent with the Langmuir isotherm. When (C/θ) was plotted *vs* inhibitor concentration (C), a straight line was noted as shown in Fig. 2. The results also indicated that the synthesized compounds, **1** and **2** could adsorb onto the mild steel metal surfaces based on the Langmuir isotherm model according to Eq. (10) [23]:

$$C/\theta = 1/K + C \quad (10)$$

where: K = is the equilibrium constant of the adsorption process.

The Tafel curves were given by the method of electrochemical parameters, which shown the corrosion rate of mild steel using hydrochloric acid (HCl) at 25 °C in the presence and the absence of inhibitors (**1** and **2**) at concentrations (1×10^{-3}, 1×10^{-4}, 1×10^{-5} M). Tafel curves were shown the values of the reaction rate (CRmpy), corrosion current (I_{corr}), corrosion potential (E_{corr}), as well as anodic and cathodic Tafel constants (βc, βa). The percentage of inhibition efficiency was calculated from the Eq. (8 and 9). The results are shown in Table 1 and 2 and Fig. 1 and 2. The results obtained from the Tafel diagram for the corrosion of carbon steel (using only HCl at 0.1 M concentration) were compared with the results obtained from the Tafel scheme by using inhibitors (**1** and **2** with the concentration 1×10^{-3} M) at 25 °C.

The results can be summarized: corrosion potential value changed from -0.739 V (presence HCl only) to -0.624 and -0.620 V (presence inhibitors compounds **1** and **2**, respectively). That means the corrosion potential became less -0.115 with inhibitor **1** and -0.119 with inhibitor **2**. The current density value decreased from 0.00233 A (when there is HCl only) to 0.000251 and 0.000203 A (when inhibitors **1** and **2**, respectively). These changes provide good evidence that inhibitors **1** and **2** reduce the corrosion rate of mild steel in the acidic medium. In addition, the corrosion rate was dropped from 3.383 mpy (using acid only) to 1.812 and 1.221 mpy in the presence of inhibitors **1** and **2**, respectively. Thus, the percentage of inhibitory efficiency became 89.22 and 91.30% at a concentration (1×10^{-3}), as shown in Table (1 and 2) and Fig. 1 and 2.

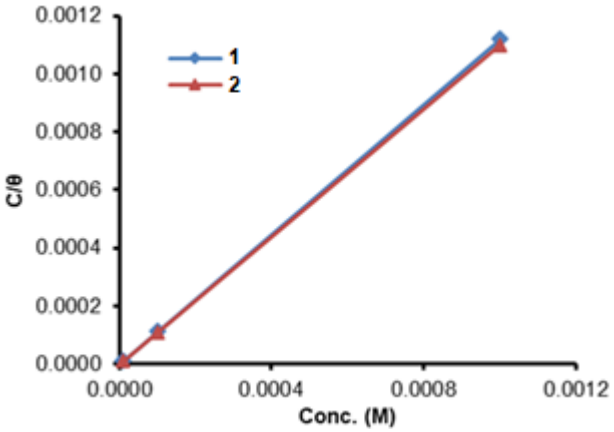

Fig 2. Langmuir adsorption isotherm model for inhibitors in 0.1 M HCl on the surface of mild steel

From the above values, we concluded that the inhibition efficiency of mild steel in an acidic medium increases with the increase in the concentration of the inhibitor due to the increase of adsorption on the metal's surface, leading to an increase in the surface area that covered by inhibitor molecules. Furthermore, the addition of inhibitors with different concentrations affected the Tafel curve shape, and the behavior of this curve works to reduce the interaction on the anode (βa) and cathode (β). Thus, these inhibitors can be considered mixed inhibitors.

Mechanism of Inhibition

From the results obtained from electrochemical, it was concluded that the (azo compounds) inhibit the corrosion of mild steel in 0.1 M HCl by adsorption at the

mild-steel solution interface. It is a general assumption that the adsorption of organic molecules may adsorb on the metal surface in three types, namely [20-21].

1. Electrostatic interaction between the charge of molecules and the charged metal.

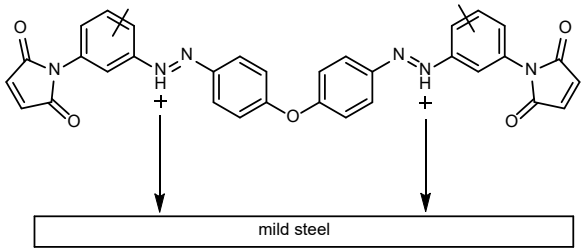

2. Interaction of unshared electron pairs in the molecule with metal.

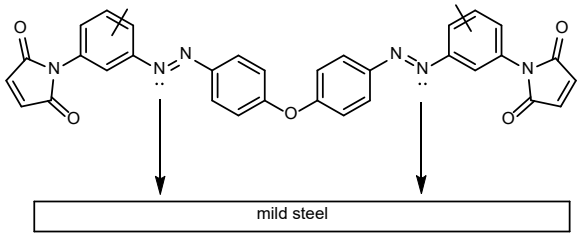

3. Interaction of pi-electrons with metal.

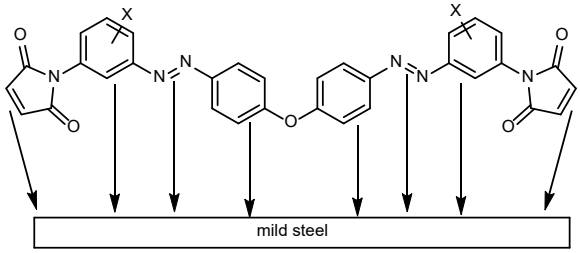

Theoretical Study

In this part, the relationship between the electronic and molecular structure and the IE of the synthesized compounds (**1** and **2**) was investigated. The molecular parameters that are relevant to the potential activity of these compounds such as the LUMO and HOMO energy, dipole moment (μ), energy gap ($\Delta E_{LUMO-HOMO}$), electron affinity (EA), ionization potential (IP), electronegativity (χ), absolute softness (σ), chemical hardness (η), number of electrons transferred (ΔN) and the global electrophilicity (ω) were extensively studied. Molecular parameter values were estimated using the DFT method and used to identify the properties and activities of the compounds under study. The above factors help to explain the values acquired with the corrosion process.

We have found that the orbital of both HOMO and LUMO values and the energy gaps observed in the chemical compounds. The literature survey revealed that the adsorption of the corrosion inhibitor compounds on the steel metal surfaces was based on the donor-acceptor interactions that locate between the π-electrons in the compounds and vacant *d*-orbitals in the surface atoms of the metallic compounds [24]. The adsorption ability of the synthesized compounds on the mild steel surfaces was attributed to their LUMO and HOMO energy values [25]. HOMO has described the ability of the molecules to donate electrons, whereas LUMO refers to their capability to accept electrons [26]. Higher E_{HOMO} and lower E_{LUMO} and $\Delta E_{LUMO-HOMO}$ values were an effective indicator of the inhibition efficiency of these compounds due to the lower energy required to remove the electrons from the occupied orbitals. Fig. 3 shows the electronic density and the geometry optimization of the LUMO and HOMO orbitals for the compounds. The results revealed that the electron-donating center was nitrogen and oxygen atoms and phenyl groups.

In comparison between compounds **1** and **2**, the data calculations showed that molecule **2** gave the maximal HOMO value and the lowest LUMO, as listed in Table 3. These results were in agreement with the experimental values. The absolute electronegativity (χ)

Table 3. Quantum chemical parameters values for the compounds **1** and **2**

Parameters	**1**	**2**
E_{HOMO} (eV)	-4.840	-4.794
E_{LUMO} (eV)	-3.472	-3.479
$\Delta E_{LUMO-HOMO}$ (eV)	1.368	1.315
μ (Debye)	1.472	3.207
IP (eV)	4.840	4.794
EA (eV)	3.472	3.479
χ (eV)	4.156	4.136
η (eV)	0.684	0.657
ω (eV)	12.626	13.011
σ (eV)	1.462	1.520
ΔN (eV)	2.079	2.177
IE% (exp.)	87.09	90.08

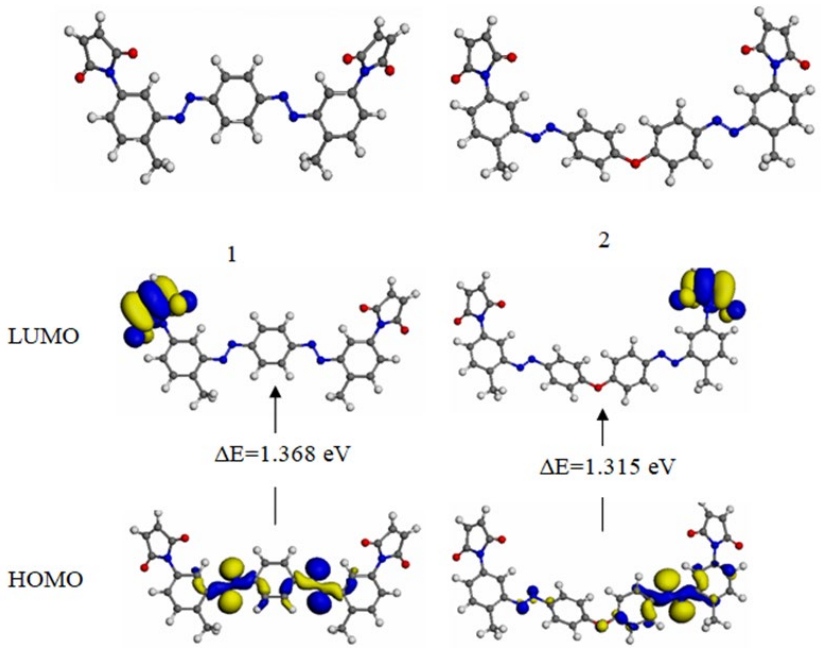

Fig 3. Geometry optimization and HOMO, LUMO orbital's of the studied compounds

and ionization potential (IP) are significant factors to describe the chemical reactivity of the molecules and atoms. Higher IP and χ values showed a higher chemical inertness and chemical stability, whereas a smaller value specified a higher reactivity of the molecules and atoms [27]. Table 3 illustrates the IP and absolute electronegativity values, confirming that compound **2** had higher inhibition efficiency (%).

Furthermore, softness (σ) and global hardness (η) are important properties to determine the reactivity and stability of the molecules. Under chemical reactions, the chemical hardness expresses the material's resistance to deformation or polarization of the electron, including ions, molecules, and atoms. Furthermore, hard molecules possess a high energy gap, whereas soft molecules display a smaller energy gap [28]. Compound **2** has the best softness and lesser hardness properties; hence, compound **2** showed a better inhibitor efficiency. Additionally, global electrophilicity (ω) was a vital reactivity marker that can be used to compare different molecules based on their electron-donating capability [29]. A higher global electrophilicity indicated that the molecules behave as an electrophile. Meanwhile, compound **2** has an electrophilic behavior and showed maximal inhibition. Similar results were noted experimentally.

According to the calculated number of electrons (ΔN) it was observed that IE (%) resulting from an electronic donation was similar to that observed by Lukovits et al. [30]. Suppose $\Delta N < 3.6$, an increase in IE was noted as the electron-donating ability of the metal surfaces increased. Thus, compounds **1** and **2** showed a higher inhibition efficiency. Hence, compound **2** showed the highest fraction of electrons that were transferred (2.177). The above results were in agreement with the experimental results.

Dipole moment (μ) is a different quantum chemical parameter that represents the corrosion IE value. This factor describes an electron distribution and bond. High values of μ (Debye) indicated that the adsorption ratio between the chemical compounds and the metal surface was high [31]. Furthermore, the deformability energy increased when the value of μ was increased, which indicated that the molecules could easily adsorb on the surface of iron (Fe) molecules. Compound **2** showed the highest dipole moment (3.207 Debye). Hence, a direct relationship was noted between the dipole moment and IE [22].

Thus, compound **2** showed higher inhibitory properties towards iron corrosion compared to compound **1**. The difference in inhibition efficiency of

compounds **1** and **2** can be due to differences in the molecular structure of inhibitors, wherein compound **2** contains an oxo-diphenyl group rather than the phenyl group in the molecular structure of compound **1**.

■ CONCLUSION

In summary, novel maleimide derivatives were synthesized as effective corrosion inhibitors. These compounds were dissolved in 0.1 M HCl solution and adsorb onto the mild steel surface at varying concentrations. The best inhibitory efficiency (IE%) values were calculated at concentration 1×10^{-3} M. These maleimide derivatives can be considered mixed inhibitors and followed the Langmuir adsorption isotherm.

Based on the theoretical analysis, the synthesized maleimide derivatives displayed corrosion inhibitory properties for the iron alloys. In addition, the IE% of maleimide derivative **2** was higher than maleimide derivative **1**, to contain derivative **2** on an oxo-diphenyl group. Furthermore, the experimental and theoretical results were in agreement.

■ ACKNOWLEDGMENTS

The authors gratefully acknowledge Dr. Ali Abd-Alimmam (Department of Chemistry, College of Science, Basrah University, Iraq) for facilitation in evaluating corrosion inhibition of synthesized maleimide derivatives.

■ AUTHOR CONTRIBUTIONS

Mohammed K. has synthesized maleimide derivatives, Hawraa K. conducted the corrosion inhibition calculations, Ashwaq S. has performed the corrosion experiments for the prepared derivatives and Rafid H. conducted the theoretical study. All authors agreed to the final version of this manuscript.

■ REFERENCES

[1] Emregül, K.C., and Atakol, O., 2003, Corrosion inhibition of mild steel with Schiff base compounds in 1 M HCl, *Mater. Chem. Phys.*, 82 (1), 188–193.

[2] Al-Doori, H.H., and Shihab, M.S., 2014, Study of some [N-substituted] p-aminoazobenzene as corrosion inhibitors for mild-steel in 1 M H_2SO_4, *Al-Nahrain J. Sci.*, 17 (3), 59–68.

[3] Dhaif, H.K., Jasim, E.Q., Muhajjar, Z.A., and Shanta, A.A., 2019, Corrosion Inhibition of Mild-Steel in 0.5 M HCl using some prepared, *Mediterr. J. Chem.*, 9 (4), 290–304.

[4] Abdallah, M., Asghar, B.H., Zaafarany, I., and Fouda, A.S., 2012, The inhibition of carbon steel corrosion in hydrochloric acid solution using some phenolic compounds, *Int. J. Electrochem. Sci.*, 7, 282–304.

[5] Jawad, A.E., and Shihab, M.S., 2017, Pyridine derivatives as corrosion inhibitors for mild steel in 1 M H_2SO_4 solution, *Iraqi J. Ind. Res.*, 4 (1), 57–66.

[6] Jasim, E.Q., Mohammed-Ali, M.A., and Hussain, A.A., 2015, Investigation of *Salvadora persica* roots extract as corrosion inhibitor for mild steel in 1 M HCl and in cooling water, *Chem. Mater. Res.*, 7 (4), 147–159.

[7] Fouda, A.S., El-Azaly, A.H., Awad, R.S., and Ahmed, A.M., 2014, New benzonitrile azo dyes as corrosion inhibitors for carbon steel in hydrochloric acid solutions, *Int. J. Electrochem. Sci.*, 9, 1117–1131.

[8] Mabrouk, E.M., Eid, S., and Attia, M.M., 2017, Corrosion inhibition of carbon steel in acidic medium using azo chromotropic acid dye compound, *J. Basic Environ. Sci.*, 4, 351–355.

[9] Abdallah, M., Alfakeer, M.M., Hasan, N.F., Alharbi, A.M., and Mabrouk, E.M., 2019, Polarographic performance of some azo derivatives derived from 2-amino-4-hydroxy pyridine and its inhibitory effect on C-steel corrosion in hydrochloric acid, *Orient. J. Chem.*, 35 (1), 98–109.

[10] Fouda, A.S., El-Morsi, M.A., Gaber, M., and Fakeeh, M., 2017, Azo compounds as green corrosion inhibitor for carbon steel in hydrochloric acid solution: Corrosion inhibition and thermodynamic parameters, *Int. J. Electrochem. Sci.*, 12, 8745–8760.

[11] Nagiub, A.M., Mahross, M.H., Khalil, H.F.Y., Mahran, B.N.A., Yehia, M.M., and El-Sabbah, M.M.B., 2013, Azo dye compounds as corrosion inhibitors for dissolution of mild steel in hydrochloric acid solution, *Port. Electrochim. Acta*, 31 (2), 119–139.

[12] Ismail, A., 2016, A review of green corrosion inhibitor for mild steel in seawater, *ARPN J. Eng. Appl. Sci.*, 11 (14), 8710–8714.

[13] Mabrouk, E.M., Shokry, H., and Al-Naja, K.M.A., 2011, Inhibition of aluminum corrosion in acid solution by mono- and bis-azo naphthylamine dyes, *Chem. Met. Alloys*, 4, 98–106.

[14] Al-Juaid, S.S., 2007, Mono azo dyes compounds as corrosion inhibitors for dissolution of aluminum in sodium hydroxide solutions, *Port. Electrochim. Acta*, 25 (3), 363–373.

[15] Mohammed, I.A., and Mustapha, A., 2010, Synthesis of new azo compounds based on *N*-(4-hydroxypheneyl)maleimide and *N*-(4-methylpheneyl) maleimide, *Molecules*, 15 (10), 7498–7508.

[16] Shihab, N.L., and Intedhar, K.M., 2013, Synthesis of some novel heterocyclic azo dyes for acridine derivatives and evaluation of their antibacterial activities, *J. Chem. Pharm. Res,* 5 (5), 345–354.

[17] Zhang, H., Shang, Y., Li, M., Zhao, H., Wang, X., and Han, B., 2015, Theoretical study on the radical reaction mechanism in the cross-linking process of polyethylene, *RSC Adv.*, 5 (110), 90343–90353.

[18] Wang, H., Wang, X., Wang, H., Wang, L., and Liu, A., 2007, DFT study of new bipyrazole derivatives and their potential activity as corrosion inhibitors, *J. Mol. Model.*, 13 (1), 147–153.

[19] Pagariya, S. K., Pathade, R. M., and Bodkhe, P. S., 2015, Synthesis , Characterization and Antimicrobial screening of some Azo compounds derived from ethyl vanillin, *Res. J. Chem. Sci.*, 5 (7), 20–28.

[20] Mohammed, M. K., Almashal, F. A., and Jassem, A. M., 2021, 1,3-Dipolar Cycloaddition: Free Catalytic Synthesis and Esophageal Cancer Activity of New 1,2,3-Triazole-Oxydianiline-Maleimide Hybrids, *Egyptian Journal of Chemistry*, 64 (1), 47–53.

[21] Liao, Q.Q., Yue, Z.W., Yang, D., Wang, Z.H., Li, Z.H., Ge, H.H., and Li, Y.J., 2011, Self-assembled monolayer of ammonium pyrrolidine dithiocarbamate on copper detected using electrochemical methods, surface enhanced Raman scattering and quantum chemistry calculations, *Thin Solid Films*, 519 (19), 6492–6498.

[22] Yousefi, A., Javadian, S., and Neshati, J., 2014, A new approach to study the synergistic inhibition effect of cationic and anionic surfactants on the corrosion of mild steel in HCl solution, *Ind. Eng. Chem. Res.*, 53 (13), 5475–5489.

[23] Amoko, S.J., Akinyele, O.F., Oyeneyin, O.E., Olayanju, D.S., and Aboluwoye, C.O., 2018, Synthesis, characterization and computational studies on the corrosion inhibitive potentials of (e)-3-(2-p-tolyldiazenyl)-1-nitrosonaphthalen-2-ol, *Leonardo J. Sci.*, 33, 29–48.

[24] Domenicano, A., and Hargittai, I., 1992, *Accurate Molecular Structures: Their Determination and Importance*, Oxford University Press, Oxford, UK.

[25] Habeeb, H.J., Luaibi, H.M., Abdullah, T.A., Dakhil, R.M., Kadhum, A.A.H., and Al-Amiery, A.A., 2018, Case study on thermal impact of novel corrosion inhibitor on mild steel, *Case Stud. Therm. Eng.*, 12, 64–68.

[26] Yousef, T.A., El-Reash, G.M.A., and El Morshedy, R.M., 2012, Quantum chemical calculations, experimental investigations and DNA studies on (E)-2-((3-hydroxynaphthalen-2-yl)methylene)-N-(pyridin-2-yl)hydrazinecarbothioamide and its Mn(II), Ni(II), Cu(II), Zn(II) and Cd(II) complexes, *Polyhedron*, 45 (1), 71–85.

[27] Agalave, S. G., Maujan, S. R., and Pore, V. S., 2011, Click Chemistry: 1,2,3-Triazole as pharmacophore, *Chem. Asian J.*, 6 (10), 2696 – 2718.

[28] Hasanov, R., Sadıkoğlu, M., and Bilgiç, S., 2007, Electrochemical and quantum chemical studies of some Schiff bases on the corrosion of steel in H_2SO_4 solution, *Appl. Surf. Sci.*, 253 (8), 3913–3921.

[29] Chattaraj, P.K., Giri, S., and Duley, S., 2011, Update 2 of: Electrophilicity index, *Chem. Rev.*, 111 (2), PR43–PR75.

[30] Lukovits, I., Kálmán, E., and Zucchi, F., 2001, Corrosion inhibitors–correlation between electronic structure and efficiency, *Corrosion*, 57 (1), 3–8.

[31] Li, X., Deng, S., Fu, H., and Li, T., 2009, Adsorption and inhibition effect of 6-benzylaminopurine on cold rolled steel in 1.0 M HCl, *Electrochim. Acta*, 54 (16), 4089–4098.